



# Spatio-temporal evaluation of remote sensing rainfall data of TRMM satellite over the Kingdom of Saudi Arabia

Sajjad Hussain<sup>1</sup> · Amro M. Elfeki<sup>1,2</sup> · Anis Chaabani<sup>1</sup> · Esubalew Adem Yibrie<sup>1</sup> · Mohamed Elhag<sup>1,3,4,5</sup>

Received: 18 April 2022 / Accepted: 17 July 2022 / Published online: 10 August 2022  
© The Author(s), under exclusive licence to Springer-Verlag GmbH Austria, part of Springer Nature 2022

## Abstract

Rainfall estimation is the most important parameter for many water resource simulations and practices; therefore, precise and long-term data are required for trustworthy precipitation depiction. Recent advancements in remote sensing applications enabled researchers to estimate rainfall with greater geographical and temporal precision. The goal of this study was to evaluate the performance of a climatological satellite, the Tropical Rainfall Measuring Mission (TRMM) in estimating rainfall, with ground-based gauge data for five years (2008–2012) across the entire Kingdom of Saudi Arabia (KSA). In regional and station-based evaluations, many statistical performance metrics such as  $R$ -square ( $R^2$ ), root-mean-squared error (RMSE), mean absolute error (MAE), relative BIAS (R.B.), and correlation coefficient (CC) have been utilized. The southern, north-western, and south-western areas performed very well in the regression and correlation analyses. The problem of under and overestimating satellite data, according to R.B. analysis, exists across the Kingdom, with the southern, eastern, and north-western areas dominating (maximum over is R.B. = 94.6% and minimum over is 7.5%, while maximum under R.B. = -52.8% and minimum under R.B. = -5.9%). The RMSE and MAE were higher in the Qassim, Jazan, and Makkah regions, whereas they were the lowest in the northwestern. In general, TRMM prominently identified rainfall in comparison with the ground-based data and performed moderately for the majority of stations and regions during the research period.

## 1 Introduction

Climate change, which has resulted in high temperatures, precipitation, floods, and global sea-level rise, is the most serious issue that has emerged in recent decades (Khan et al. 2010; Swain et al. 2020). Severe weather conditions are prevalent over the world, causing flooding and significant infrastructure damage (Seyyedi et al. 2014; Awais et al.

2021). So, there is a need for a long-term and accurate precipitation dataset to examine the climate simulation model and other hydrological studies (Moazami et al. 2013; Tapiador et al. 2017; Lu and Yong 2018; Ricciardelli et al. 2018). Most essential phenomena, including ground-water recharge assessment, and flood and drought monitoring, need precipitation as input parameters, indicating its importance in water resources (Behrangi et al. 2011; Su et al. 2011; Jiang

✉ Mohamed Elhag  
melhag@kau.edu.sa

Sajjad Hussain  
smuhammadsingle@stu.kau.edu.sa

Amro M. Elfeki  
aelfeki@kau.edu.sa

Anis Chaabani  
achaabani@kau.edu.sa

Esubalew Adem Yibrie  
eyibrieismail@stu.kau.edu.sa

<sup>2</sup> Irrigation and Hydraulics Department, Faculty of Engineering, Mansoura University, Mansoura, Egypt

<sup>3</sup> Department of Geoinformation in Environmental Management, CI-HEAM/Mediterranean Agronomic Institute of Chania, 73100 Chania, Greece

<sup>4</sup> The State Key Laboratory of Remote Sensing, Aerospace Information Research Institute, Chinese Academy of Science (CAS), Beijing 100101, China

<sup>5</sup> Department of Applied Geosciences, Faculty of Science, the German University of Technology in Oman, Muscat 1816, Oman

<sup>1</sup> Department of Hydrology and Water Resources Management, Faculty of Meteorology, Environment & Arid Land Agriculture, King Abdulaziz University, Jeddah 21589, Saudi Arabia

et al. 2012; Bahrawi et al. 2021). Precipitation estimate has traditionally been done using on-ground rain gauges, which give real-time details regarding rainfall occurrence but not geographically dispersed data (Artan et al. 2007; Alharthi et al. 2020). Long-term and continuous data gauge monitoring systems will also necessitate a significant financial and technological commitment. Rainfall quantification is difficult to estimate because of unequal distribution or geographical inhomogeneity, especially when data collecting by the ground station is scarce (Gu et al. 2010; Camberlin et al. 2019). Rainstorms also have a lot of spatial unevenness in dry and semi-arid environments, especially when the rainfall intensity is strong (Habib and Nasrollahi 2009; Farran et al. 2021). As a result, sensor-based precipitation estimates are becoming increasingly promising in recent years, with satellite sensors dominating because of their greater regional coverage and temporal precision (Maggioni and Massari 2018; Hussain et al. 2022; Bahrawi and Elhag 2020). The data available from various sources are currently being employed to understand precipitation patterns on a global and regional scale (Collischonn et al. 2008; Poinot 2020). The advantages of satellite-based measurements include non-disturbed coverage in areas where ground-based gauges cannot install, specifically in the hilly and oceanic regions (De Coning 2013; Gado et al. 2017; Awais et al. 2022). Several satellites, including the Climate Prediction Center morphing technique (CMORPH), the Tropical Rainfall Measuring Mission (TRMM), the Multi-satellite Precipitation Analysis (TMPA), the Global Precipitation Measurement (GPM), and the Precipitation Estimation from Remotely Sensed Information Using Artificial Neural Networks (PERSIANN), have been launched to cover global climatic conditions (Kummerow et al. 1998; Joyce et al. 2004; Elhag et al. 2021b). Although the data obtained from these satellite products were good, they were flawed owing to random and systematic errors mostly connected to their retrieval technique and observation; therefore, they must constantly be compared to ground-based real-time data for adjustments (Segond et al. 2007; Habib et al. 2014; Fang et al. 2015; Vu et al. 2018). TRMM satellite was launched in 1997 to estimate moderate to heavy rainfall and has since gathered extensive measurements through its precipitation radar (P.R) system to provide an understanding of precipitation distribution. This spaceborne satellite is capable of covering high-resolution vertical precipitation profiles from global to ground scale (Kozu et al. 2001; Gupta et al. 2021). Saudi Arabia has a land area of roughly 2,250,000 km<sup>2</sup>, necessitating a large number of rainfall measuring locations. However, current low-density rain gauges across the country are insufficient to get an accurate spatial distribution of rain (Almazroui 2011; Elhag et al. 2021a). Consistently altering land use and high rainfall intensities can swiftly generate flash floods during or after the rainstorm, causing significant infrastructure damage (Abera

et al. 2016). Numerous researches were conducted to evaluate the performance of rainfall estimation by different satellite sensors. Choubin et al. (2019) constructed a BIAS correction framework for TRMM Satellite in which a correction factor has been established for gauged and ungauged pixels providing satisfactory results. Gauged pixels gain 57% BIAS correction while ungauged got the value of 25%, indicating significant improvement in remotely sensed precipitation estimation (Choubin et al. 2019). Dinku et al. (2010) investigated the validation of satellite rainfall for several locations in Colombia and found that the PERSIAN and GSMaP-MVK products, respectively, overestimated and underestimated their values (Dinku et al. 2010). Jiang et al. (2018) compared two high-resolution satellites, TRMM and CMORPH, for estimating precipitation over Shanghai. They found that CMORPH is more accurate than TRMM, but that it underestimates readings in particular intensity ranges (Jiang et al. 2018). Likewise, Almazroui (2011) presented a study on the calibration of TRMM data in contrast with rain gauges for the period of 10 years (1998–2009) on KSA which indicated that TRMM and rain gauge data had a higher level of significance. Precipitation measured by satellite is 92% accurate which showed an error of 8% in its measurement, so for correction of TRMM value correction factor of 0.93 has been defined in that article (Almazroui 2011). Haile et al. (2011) conducted a study and found that the CMORPH satellite has great capability for finding high spatio-temporal ( $8 \times 8$  km<sup>2</sup> — daily) rainfall (Haile et al. 2015). Mahmoud et al. (2018) conducted a study on Integrated Multi-satellite Retrievals for Global Precipitation Measurement (GPM) mission (IMERG) and analysis precipitation data on the region of Saudi Arabia. He tested the product on early, late, and final rainfall runs and discovered that it provided correct results in certain locations but inaccurate results in others. Following these evaluations, we can see that some tweaks or corrections to remotely sensed data are required in order to get more accurate precipitation data for TRMM (Mahmoud et al. 2018).

The major emphasis of this study was on the evaluation and accuracy assessment of satellite-measured precipitation (TRMM 3B43) for both station and regional levels. The novelty of this work is that it uses in-depth several error measures, namely, relative BIAS (R.B.), root-mean-square error (RMSE), mean absolute error (MAE), correlation coefficient (CC), and coefficient of determination ( $R^2$ ) on regional and station scales to evaluate the TRMM performance throughout Saudi Arabia. Furthermore, the limitations that result in larger R.B. and low correlation values were also analyzed. This study will provide a platform for arid-region researchers to better comprehend the quality of remotely sensed data on a larger scale and identify the restrictions that lead to low satellite data accuracy and serve as a foundation for object-oriented activities such as flood monitoring, drought management, and other hydrological processes.

## 2 Material and methods

### 2.1 Study area

The research covered the whole KSA from 34°32'00" to 55°40'00" in latitude and from 16°22'00" to 32°15'00" in longitude as represented in Fig. 1. Based on administrative division, KSA is subdivided into thirteen regions: Madinah, Makkah, Riyadh, Qassim, Tabuk, Asir, Jazan, Najran, Al-Jouf, Hail, Al-Baha, and Eastern and Northern Region as shown in Table 1.

The temperature is high throughout the year in the most remote portions of the Kingdom, with moderate winds, but meteorological features vary greatly from season to season. Heavy rainstorms occur just a few days a year in some sections of the state, making it the driest in the world. The majority of the land is made up of desert impermeable sections that have a limited ability to absorb precipitation

and can result in flash floods even with ordinary rainfall (Abdullah and Al-Mazroui 1998; Bahrawi et al. 2020). Most of the rainfall events occur in summer, which mainly causes the northward advancement of the southwesterly monsoon and results in nearly 300 mm, which is 60% of the annual occurrence from October to March (ŞEN and Al-Suba'i 2002).

The majority of precipitation falls on the high topographical regions and mountainous slopes, whereas rainfall in the rest of the country is modest and uneven, with high intensities and short durations. Rainfall variability patterns locally or regionally based on the resulting impact of El Niño Southern Oscillation (ENSO), the North Atlantic Oscillation (NAO) patterns (Almazroui 2011; Hasanean and Almazroui 2015). The average annual rainfall in most arid regions is less than 100 mm, whereas mountainous places receive more than 300 mm. (Hag-elsafi and El-Tayib 2016).

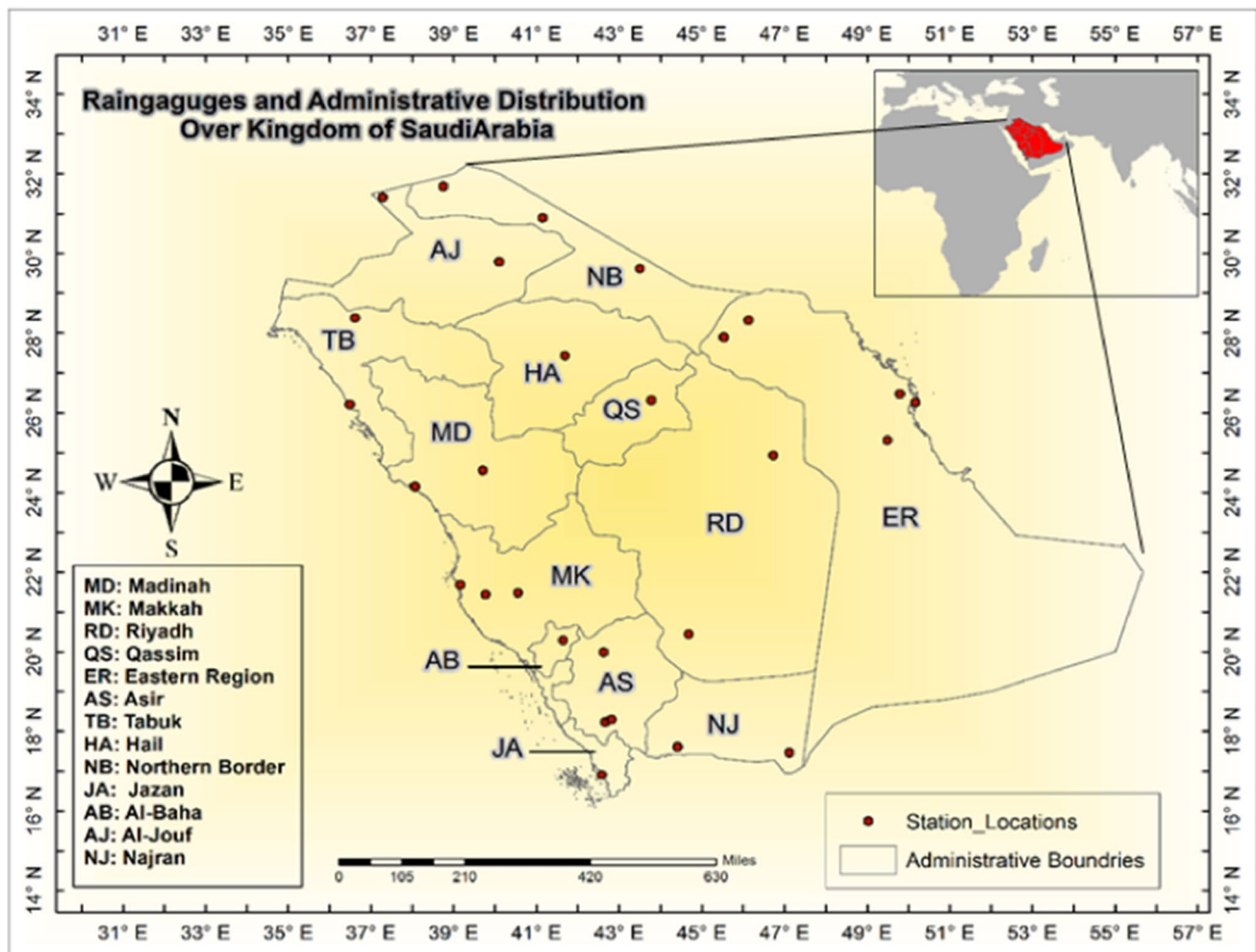


Fig. 1 Location of the study area and the administrative regions of the Kingdom of Saudi Arabia

**Table 1** Rain gauges considered in the study

Region no	ID	Region	Station	Elevation (m)
1	AS	Asir	Abha	2102
			Khamis Mushait	2060
			Bisha	1171
2	NJ	Najran	Najran	1217
			Sharorah	727
3	JA	Jazan	Jazan	5
4	AB	Al-Baha	Baha	1600
5	MK	Makkah	Taif	1457
			Makkah	261
			Jeddah	5
6	RD	Riyadh	Riyadh	614
			Wadi Dawasir	702
7	ER	Eastern Region	Hafar Al-Batin	415
			Qaisumah	358
			Al-Ahsa	178
			Dhahran	21
			Dammam	14
8	MD	Madinah	Madinah	639
			Yanbu	12
9	AJ	Al-Jouf	Jawf	673
			Qurayyat	510
10	TB	Tabuk	Tabuk	768
			Wajh	15
11	HA	Hail	Hail	1006
12	NB	Northern Border	Arar	550
			Rafha	450
			Turaif	855
13	QS	Qassim	Qassim	650

## 2.2 Data acquisition

### 2.2.1 Rain gauge dataset

Rain gauges are considered the reference for precipitation measures because of their provision for real-time rainfall estimation. In this research, data from all thirteen regions have been collected from the Ministry of Environment, Water and Agriculture (MEWA) Saudi Arabia, for 5 years from January 1, 2008, to December 31, 2012 (website: <https://www.mewa.gov.sa/en/Pages/default.aspx>, accessed on March 2020). Twenty-eight regional stations have been selected in thirteen regions for data collection covering the whole KSA (see Table 1). The 28 stations were taken under consideration for data comparison and evaluation. The graphical representation of station data for each year was prepared by intensity distribution weightage (IDW) in GIS to understand the rainfall distribution pattern visually (see Fig. 2).

### 2.2.2 Satellite dataset

Tropical rainfall measuring mission (TRMM-3B43) satellites were used to acquire precipitation datasets for this study. The satellite recorded precipitation with an extent of 50 S to 50 N, with a spatial resolution of 0.25° (Liu et al. 2012). TRMM measured rainfall using a variety of sensors, including visual, infrared, and microwave imagers (see Table 2). The sensors worked together to offer a more accurate rainfall estimate (Kummerow et al. 2000; Elhag and Yilmaz 2021). TRMM gives a greater spatial extent of rainfall distribution for the kingdom than point data provided by ground stations (see Fig. 3). Satellite data was accessible in near real-time (3 h), with the daily and monthly temporal resolution, allowing accurate rainfall monitoring. Precipitation data were obtained from the online data source of NASA for the period of 5 years 2008–2012 (website: <https://disc.gsfc.nasa.gov>, accessed on March 2020).

## 2.3 Data processing

Several pre-processing process steps were involved prior to the evaluation of the TRMM and ground datasets. The process begins with the acquisition of gauge and satellite data from their respective sources. Different procedures were adopted in Geographical Information System (GIS) ArcMap 10.5 to enable our satellite data for further interpretation (see Fig. 4). The data downloaded from the NASA website was in.nc4 file format, which needs to be converted in a more accessible processing form; therefore, data is then converted to Geotiff files by python designed tool (SMD) in ArcMap environment.

Ground control points (GCPs) were selected in order to extract TRMM pixel values from raster images. Station coordinates were obtained in Universal Transverse Mercator (UTM) format from decimal degrees for working convenience using UTM converter (<http://www.utmconverter.com>). A coordinate matching process (CMP) was applied to the gauge points in order to ensure exact value retrieval. Following the abstraction of rainfall values, a correlation to TRMM monthly rainfall with ground data was constructed on a regional and individual station basis.

## 2.4 Data comparison and evaluation

The study's comparison stage was built on the foundation of the station and regional assessments. In the second stage of the investigation, individual station data was reviewed to establish TRMM's overall dependability. There were four main statistical parameters used to evaluate TRMM dataset from which the first three parameters, including root-mean-squared error (RMSE), mean absolute error (MAE), and relative BIAS (R.B.), were described as the error within



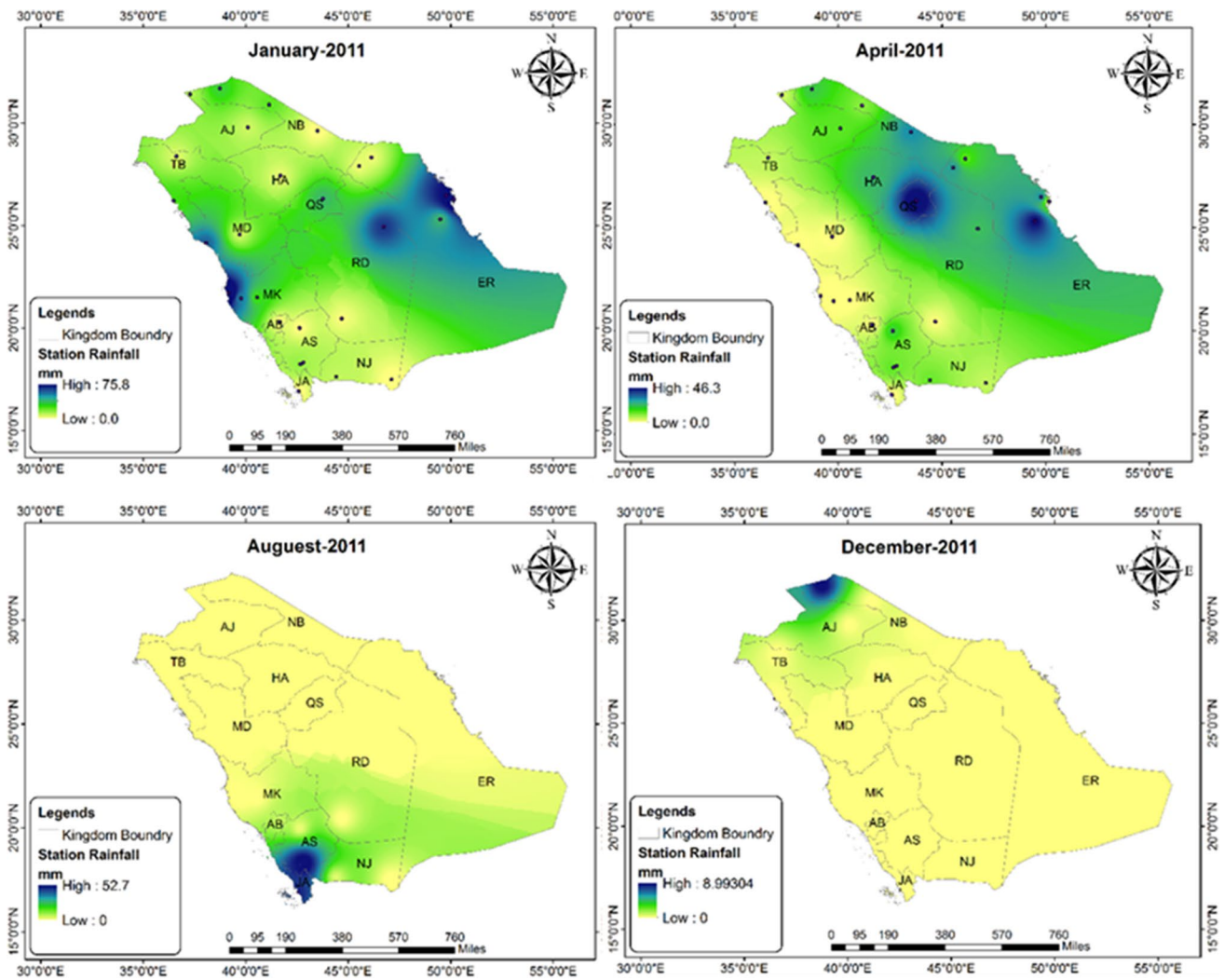


Fig. 2 Sample representation of station rainfall distribution pattern of January, April, August, and December for the year 2011 over KSA by inverse distance weighting (IDW)

Table 2 Typical information of TRMM instruments

Name of the instrument	Band frequencies	Swath width (km)	Spatial resolution (km)
Infrared and visible scanner	5 channels 12, 10.8, 3.75, 1.6, 0.63 ( $\mu\text{m}$ )	833	2.4
Microwave imager	5 frequencies (10.7, 19.4, 21.3, 37, 85.5 GHz)	878	5.1
Precipitation radar	13.8 GHz	247	5
Lightning image sensor	0.7774 $\mu\text{m}$	668	4.3

the satellite data. In contrast, the second group containing correlation coefficient and regression provides information regarding the extent of agreement between both data (see Table 3).

### 3 Results and discussion

The current research is based on comparing TRMM satellite rainfall data to ground-based measurements. Most of the study area got much lower rainfall throughout the years, indicating it was an arid environment. The maximum rainfall observed by the gauges and satellite during the whole study period was 117 and 120 mm/month, respectively, and there were lots of months in each region when no precipitation occurred. As per ground observations, the southern region, particularly Abha, had the highest average rainfall, while the

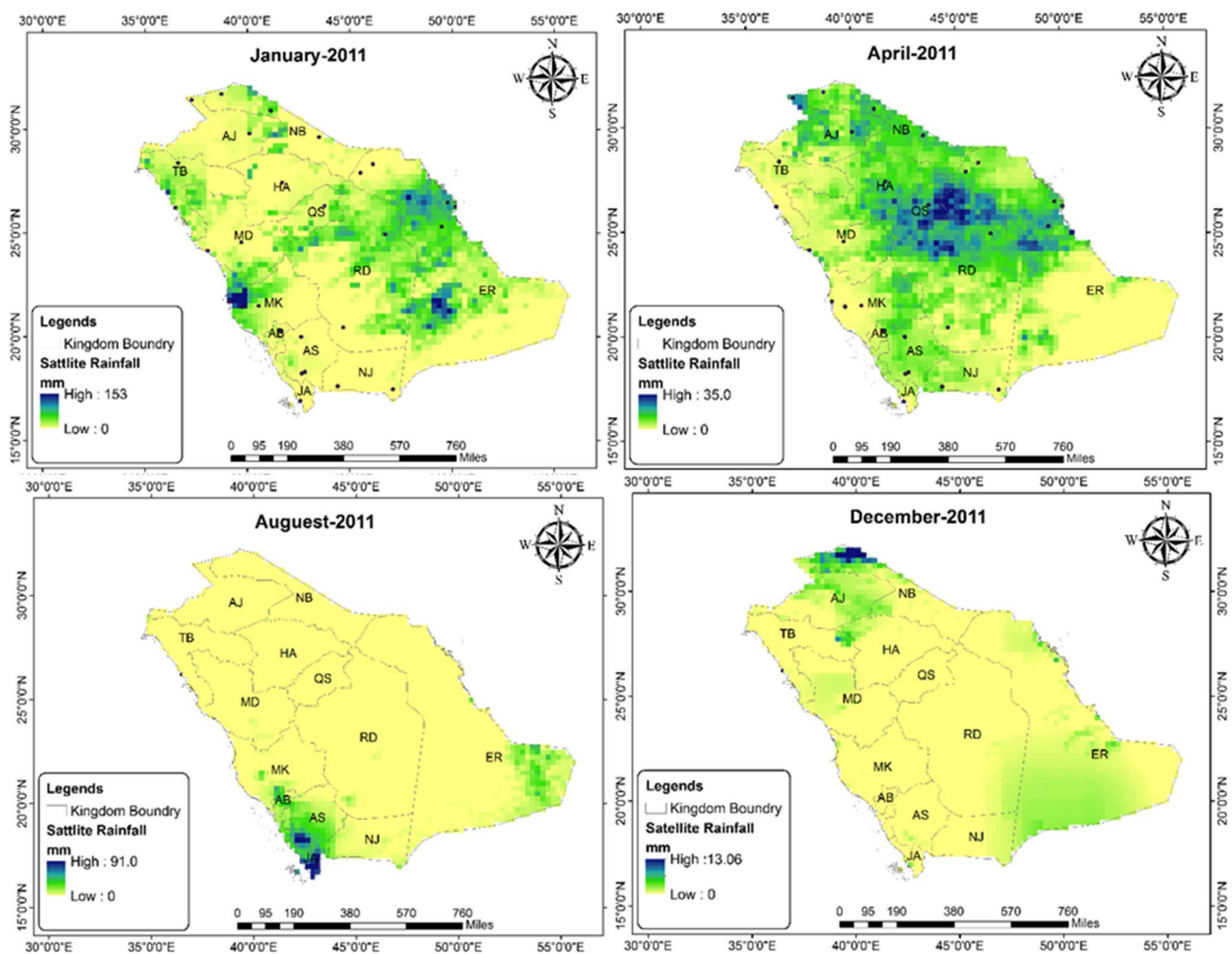


**Fig. 3** Sample representation of TRMM rainfall distribution pattern of January, April, August, and December for the year 2011 over KSA

north-western area like Arar, Jawf, and Tabuk had the lowest throughout the years. The satellite spatio-temporal pattern was also found to be similar to the ground observation spatio-temporal pattern for almost all regions (Figs. 2 and 3).

Most rainfall events occurred in winter (December–January) and summer (April–May) with higher intensities. Figure 5 shows a sample representation of the time series of Abha and Riyadh stations to demonstrate the similarities and dissimilarities between the two data sets. Visually, the figure shows relatively reasonable similarities.

### 3.1 Regional evaluation

The study was conducted to evaluate the performance of TRMM satellite rainfall for 5 years (2008–2012) on a regional scale. Statistical parameters were applied to test the reliability of satellite datasets over the Kingdom.

Regression analysis was applied to each region in order to assess the degree of agreement between stations within each

region (see Fig. 6), starting with the southern part, which includes Asir, Jazan, and Najran. The behavior is similar, with  $R^2$  values of 0.67 and 0.60 for Asir and Najran, respectively; however, it drops for Jazan to 0.40. Makkah and the Al-Baha area, both of which are located in the south-western part of the Kingdom, have regression coefficients ( $R^2$ ) of 0.61 and 0.51, respectively. Similarly, the eastern area comprises five stations (Hafar Al-Batin, Qaisumah, Dammam, Al-Ahsa, and Dhahran) and shows an average  $R^2$  of 0.58. The performance of the Madinah province is superior, as seen by the region's  $R^2$  of 0.69. Moving toward the north-western part of the country, three areas can be found: Tabuk, Hail, and Al-jouf, which provide values of  $R^2$  equal to 0.80, 0.69, and 0.59, respectively.

The value of  $R^2$  in the northern part of the Kingdom (Northern Border) was up to 0.55, suggesting fair performance. However, Qassim, which is close by, did not have a significant relationship and gained a value of 0.29 for the recorded years. The correlation was found better in the North

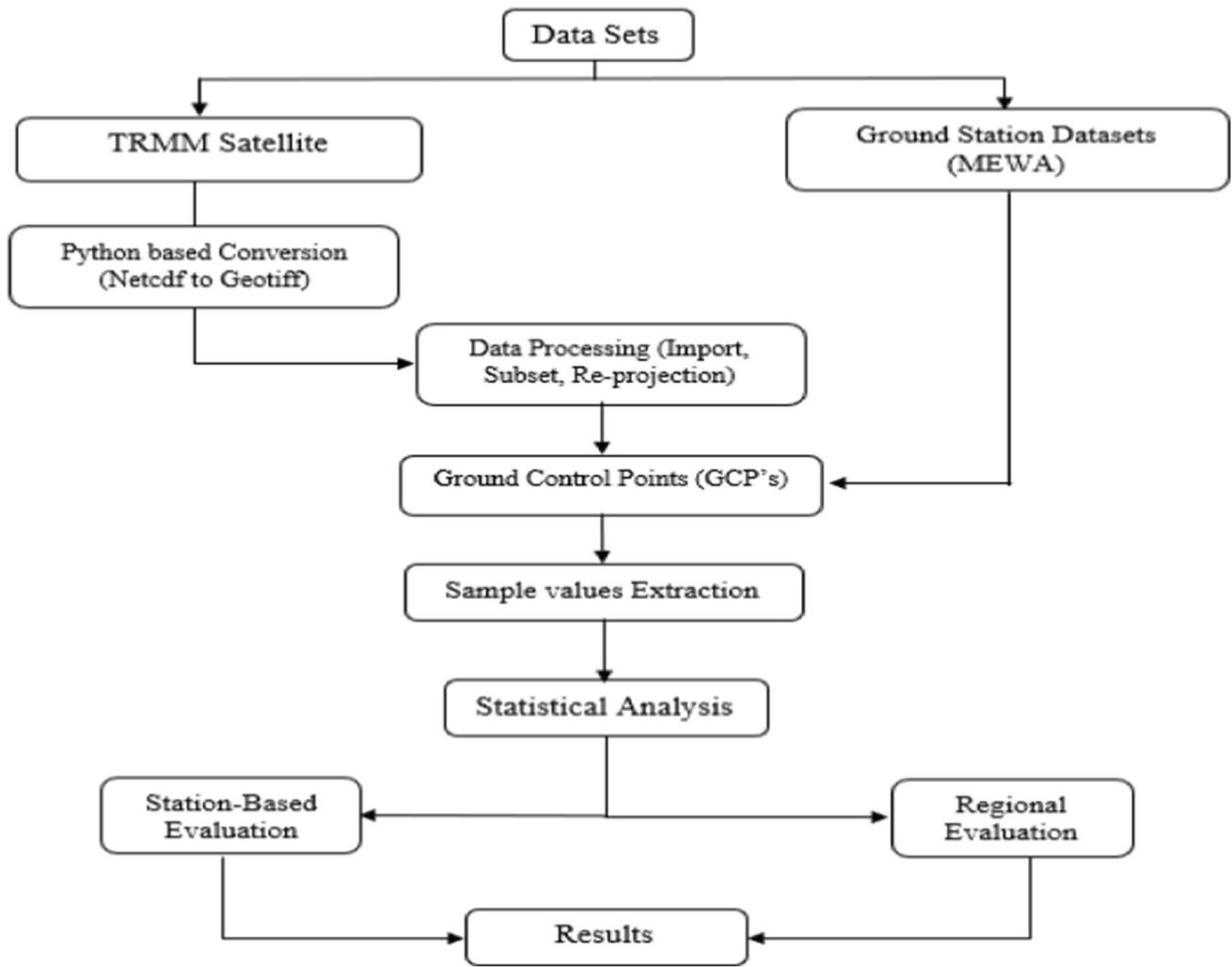


Fig. 4 Evaluation methodology flowchart

Table 3 Statistical measures

Statistical model name	Equation	Applications
Root-mean-squared error (RMSE)	$\sqrt{\frac{1}{n} \sum_{i=1}^n  X_i - Y_i }$	The express error between rain gauge and satellite data
Mean absolute error (MAE)	$\frac{1}{n} \sum_{i=1}^n  X_i - Y_i $	
Relative BIAS (R.B.)	$\frac{\frac{1}{n} \sum_{i=1}^n (X_i - Y_i)}{\sum_{i=1}^n Y_i} \times 100$	Describe the extent of agreement between satellite and gauges
Coefficient of correlation (CC)	$\frac{\frac{1}{n} \sum_{i=1}^n (X_i - \bar{X})(Y_i - \bar{Y})}{\sigma_x \sigma_y}$	
Coefficient of determination (R <sup>2</sup> )	$1 - \frac{SS_r}{SS_T}$	

$X_i$  is the observed dataset values,  $Y_i$  is the satellite dataset values,  $\bar{X}$  is the mean of the observed data set,  $\bar{Y}$  is the mean of the satellite data set,  $n$  is the sample size, and  $\sigma_x, \sigma_y$  are the standard deviation for gauge and satellite data, respectively.  $SS_r$  represents the sum of the square of regression, and  $SS_T$  indicates the total sum of squares.

(Tabuk, Hail, Madinah) and Asir regions. However, Riyadh and Qassim, showed a very low correlation (less than 0.50), indicating low assessment accuracy in these areas, while a moderate correlation was found in the eastern and north-eastern regions (see Fig. 7a).

In Makkah, Jazan, and Qassim regions, the RMSE revealed a higher degree of error, suggesting a very low satellite accuracy, with errors of 13.16 mm, 14 mm, and 17.34 mm respectively. Whereas the Riyadh, Eastern, and Asir provinces did better than the previous regions, their inaccuracy ranged from 9.44 to 9.62 mm. Al-Baha and Najran did well on the south-western and southern sides, whereas Madinah performed modestly on the western side, with an inaccuracy of 6.79 to 7.69 mm, respectively. The northern and northwestern areas of the Kingdom had substantially lower degrees of RMSE, which did not surpass 5 mm. Satellite measurements did well in most portions of Saudi Arabia except in Qassim, Jazan, and Makkah (see

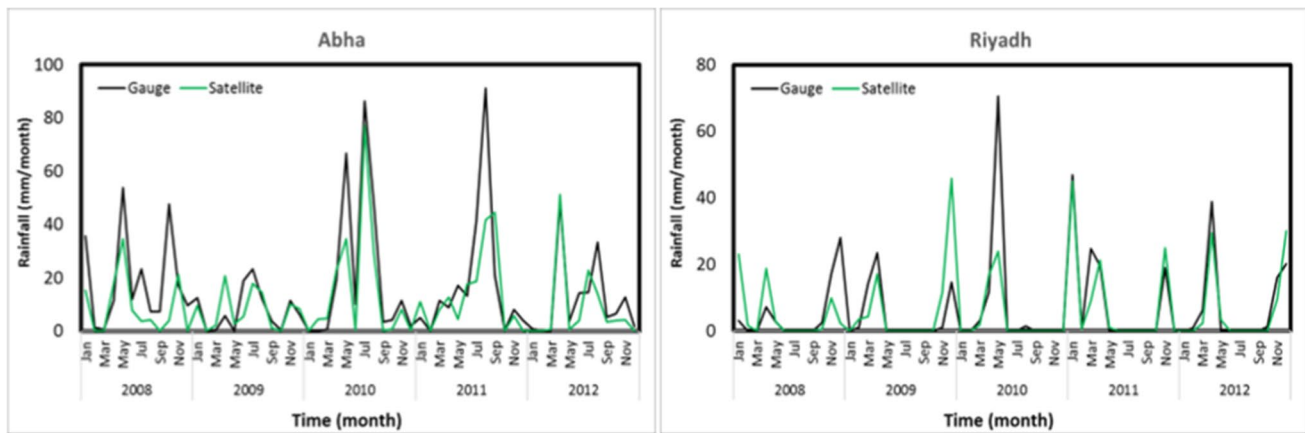


**Fig. 5** Sample representation of the time series of the rainfall of the satellite and gauge data for Abha and Riyadh stations

Fig. 7b). Maximum MAE values were found in Makkah, Qasim, and Jazan, ranging from 6.24 to 6.72 mm. Meanwhile, moderate errors of 4.04 and 5.06 mm were observed in Riyadh and Asir, indicating poor satellite performance in these locations. The Northern, North-Western, and Eastern Regions, on the other hand, significantly improved MAE from 2.18 to 3.60 mm, except for western sections and Qassim, where MAE was found to be moderately low (see Fig. 7c). For each region, the R.B. was determined (see Fig. 7d). The findings revealed that the satellite overestimated rainfall up to 52.38% in Madinah, Tabuk, Hail, Al-jouf, and Qassim. Similarly, in several areas, such as the Eastern region, Jazan, Al-Baha, and Riyadh overstated values by more than 40%. The northern border and Najran, on the other hand, were likewise underestimated, although only by a factor of 10%

### 3.2 Station-based evaluation

Statistical evaluation was applied to each station separately to evaluate the satellite response at the station scale. Interpolation was done using the inverse distance weighting (IDW) approach in Geographic Information Systems (GIS) software to assess the variability of the statistical measures spatially. The functional relation between the satellite and the ground station was investigated using the statistical metrics such as the  $R$ -squared, correlation coefficient, RMSE, MAE, and R.B. (see Fig. 8a-d). According to station-based regression analysis, six stations across the Kingdom had values equal to and more than 0.80, in some regions like the eastern, southern, and south-western. Meanwhile, some regions were found to have moderate  $c$  ranges between 0.60 and 0.80, and most of them are situated on the southern, western, and northern-western sides (Elhag et al. 2020). Numerous stations in the research area had poor satellite performance ( $R^2 < 0.60$ ), with Wadi-Dawasir and Qaisumah

stations having the least regression of 0.20 and 0.28, respectively, over the whole study period (see Table 4 for detailed values of  $R^2$  for each station with regression equations). The correlation coefficient (CC) was found to be high in the southern, eastern, and north-western stations from which five stations (Bisha, Turaif, Dhahran, Damam, and Al-Ahsa) with  $CC > 0.9$ . Similarly, nine stations, the majority of which are located in the Makkah, Madinah, and Asir areas, have a CC ranges between 0.80 and 0.90. Southwestern, north-western, and two stations from the northern border have CC ranges between 0.60 and 0.80 indicating moderate correlation. Sharorah, Wadi Dawasir, Qaisumah, Qurayyat, and Qassim stations provide a lower correlation (less than 0.6). However, overall, most of the observing sites showed an acceptable correlation between satellite and ground observation. In station-based evaluation, RMSE displayed a higher degree of error in Makkah, Qassim, Jazan, and Qaisumah stations, ranging between 13.57 and 18.35 mm. Meanwhile, nine stations in the Kingdom exhibited moderate error (12.78–8.33 mm) from which Abha, Jeddah, Wajh, and Taif were dominated with a higher degree of error (up to 10.3 mm), and the rest of the stations has a minor error (RMSE = 8.33–9.87 mm).

In general, the central (Qassim), southern (Jazan, Abha), and south-western (Makkah) stations of the country have higher values of RMSE. Mean absolute error (MAE) results were found in most of the stations (21) less than 5 mm except in the south-western part (Makkah), southern part (Jazan, Abha), and the central part (Qassim) region where values range between 5 and 8.7 mm. Likewise, the R.B. results depicted that the TRMM satellite provides under and over-estimation for the whole Kingdom. There were sixteen stations with underestimated values, of which 12 had R.B. values of more than 25%, and the majority of them were located in the north to the north-western part of the country; nevertheless, Bisha, Sharorah, and Jeddah had the same



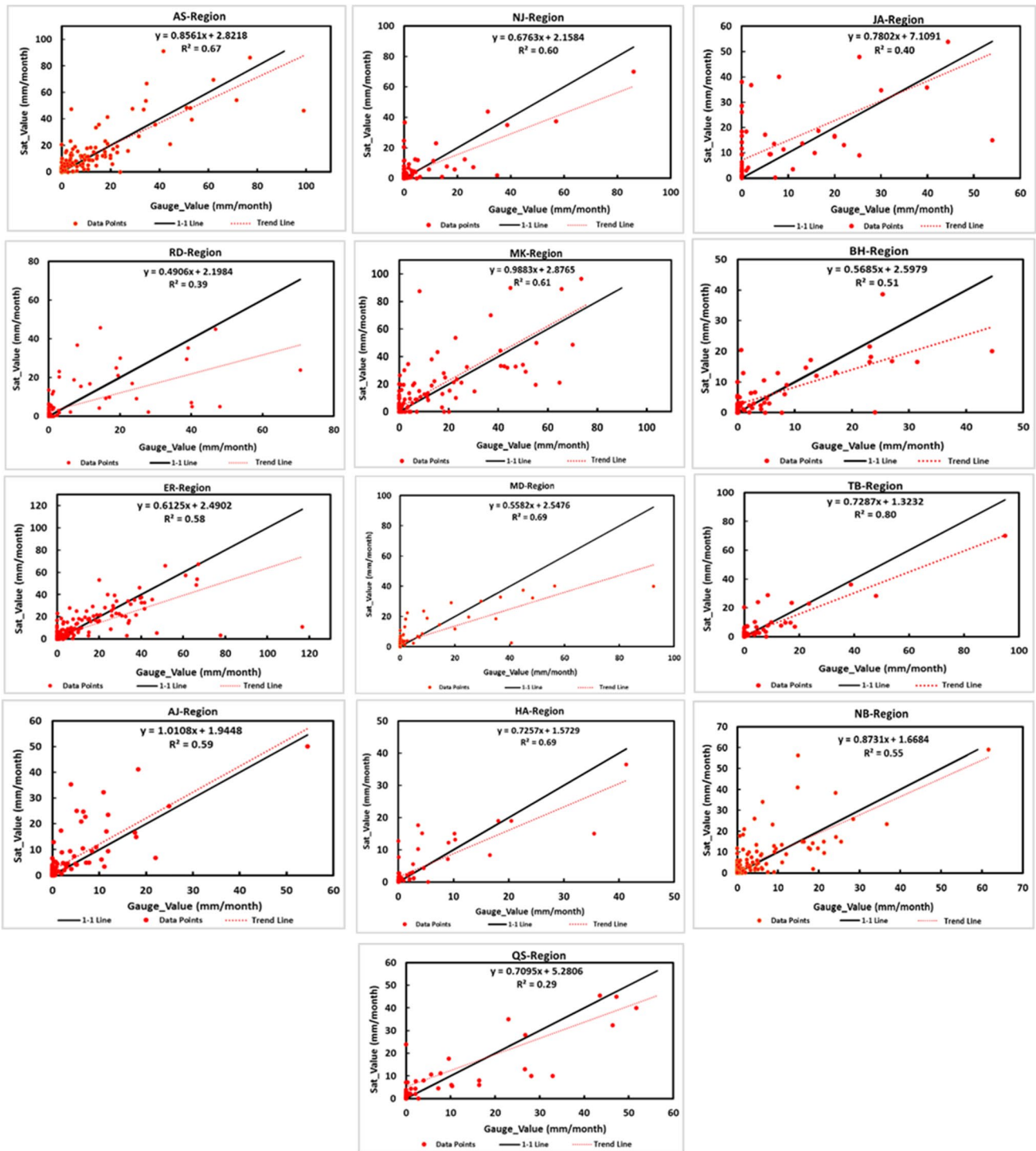
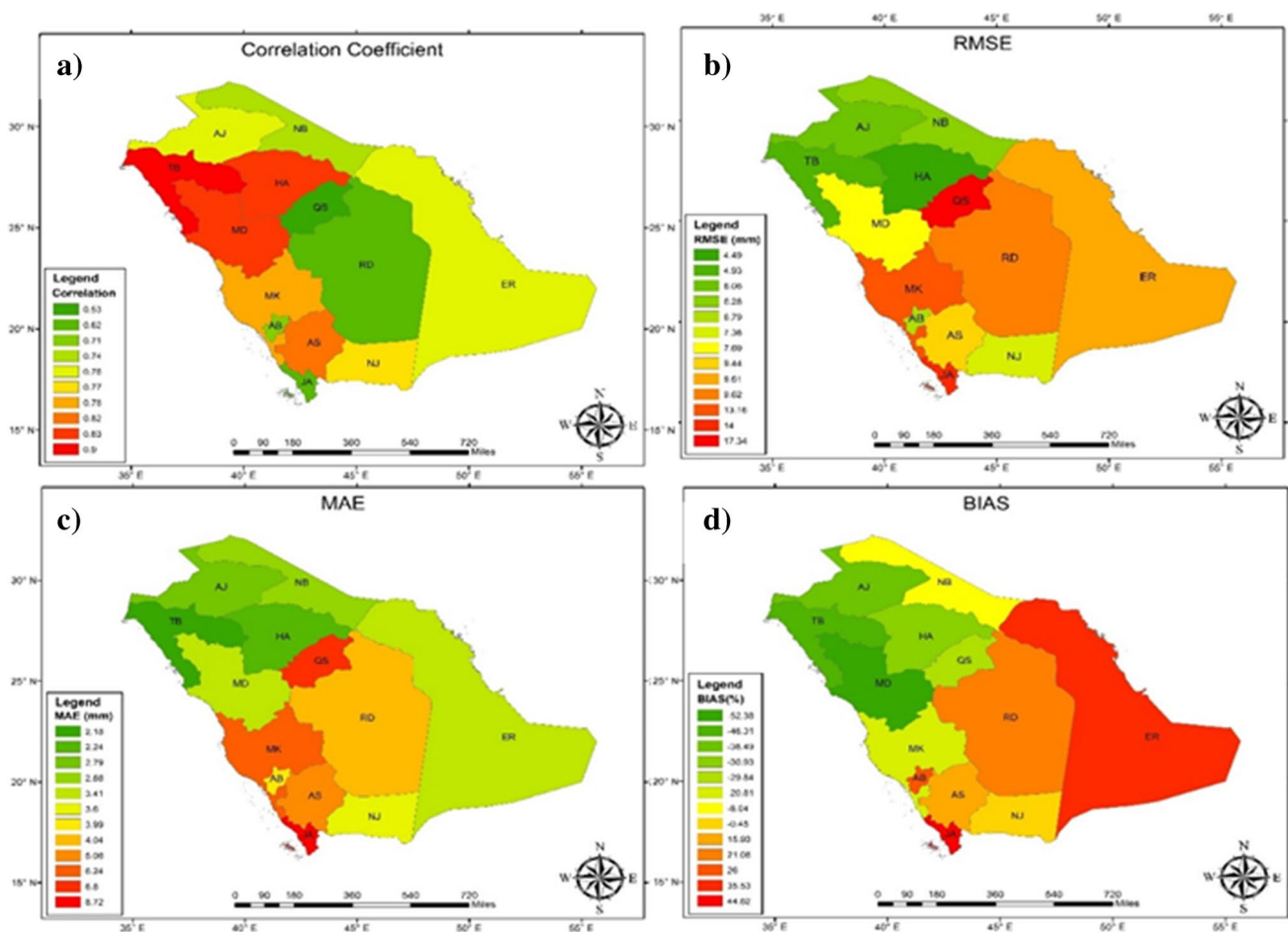


Fig. 6 Scatter plot and regression analysis of rainfall data of the stations within each administrative region of KSA

behavior but on the southern side. Taif, Makkah, Al-Ahsa, and Qurayyat all had lower R.B. values below 25%.

The south and south-western stations mainly overestimated the precipitation, and most of them range between 25 and 50% except Abha, which touches the values of 68%. The maximum fluctuation was noticed in the eastern region,

where R.B. went to 94% in Hafar Al-Batin. There were some stations (8) that showed an underestimation of less than -20%, from which Makkah, Wadi-Dawasir, Qurayyat, Rafha, and Turaif reached an overestimation of less than 10%. Overestimation and underestimation were dominating for the stations.



**Fig. 7** Administrative region-based spatial distribution of the statistical performance measure between rainfall ground stations and TRMM: **a** CC, **b** RMSE, **c** MAE, and **d** BIAS

Remotely sensed data were examined throughout the research to determine the causes of stations' and regions' poor performance (Elhag et al. 2017). It was detected that the elevation had a relationship with the value of  $R^2$  during the studied period. Low elevations up to about 261 m and elevations between 786 and 2102 m have a relatively high value of  $R^2=0.7$  on average. However, from elevations 358 to 768 m, there is a relatively low  $R^2=0.25$  on average except at elevation = 639 m. The values of  $R^2$  versus the elevations are presented in Fig. 9.

The high  $R^2$  with elevated areas using the sensors of the TRMM satellite has been reported in the literature by Xiaojun et al. (2021). However, they claimed that low  $R^2$  is reported in plain areas which does not match our results (Elhag 2016). Overall, for the entire study period in the whole Kingdom, regression analysis provided  $R^2=0.56$  indicating an average approximation of TRMM satellite with ground-based data (see Fig. 10). Based on the statistical parameterization obtained from the TRMM rainfall data, it is recommended to use these results for hydrological processes

like drought estimation using monthly rainfall depth because of its better spatial distribution and average performance over Saudi Arabia. For future research, it is recommended that this work could be extended with higher temporal resolution and detection likelihood for extreme events be taken into consideration and suggested to be extended with longer duration and dense observatories (Psilovikos and Elhag 2013).

## 4 Summary and conclusions

This research mainly focused on evaluating the Tropical Rainfall Measuring Mission (TRMM) satellite by taking rain gauge observation as a reference over the entire Kingdom of Saudi Arabia for 5 years from January 2008 to December 2012 on a monthly time scale. The evaluation was performed using statistical performance indicators, namely,  $R^2$ , RMSE, MAE, R.B, and CC. There were two major components in the evaluation, namely,

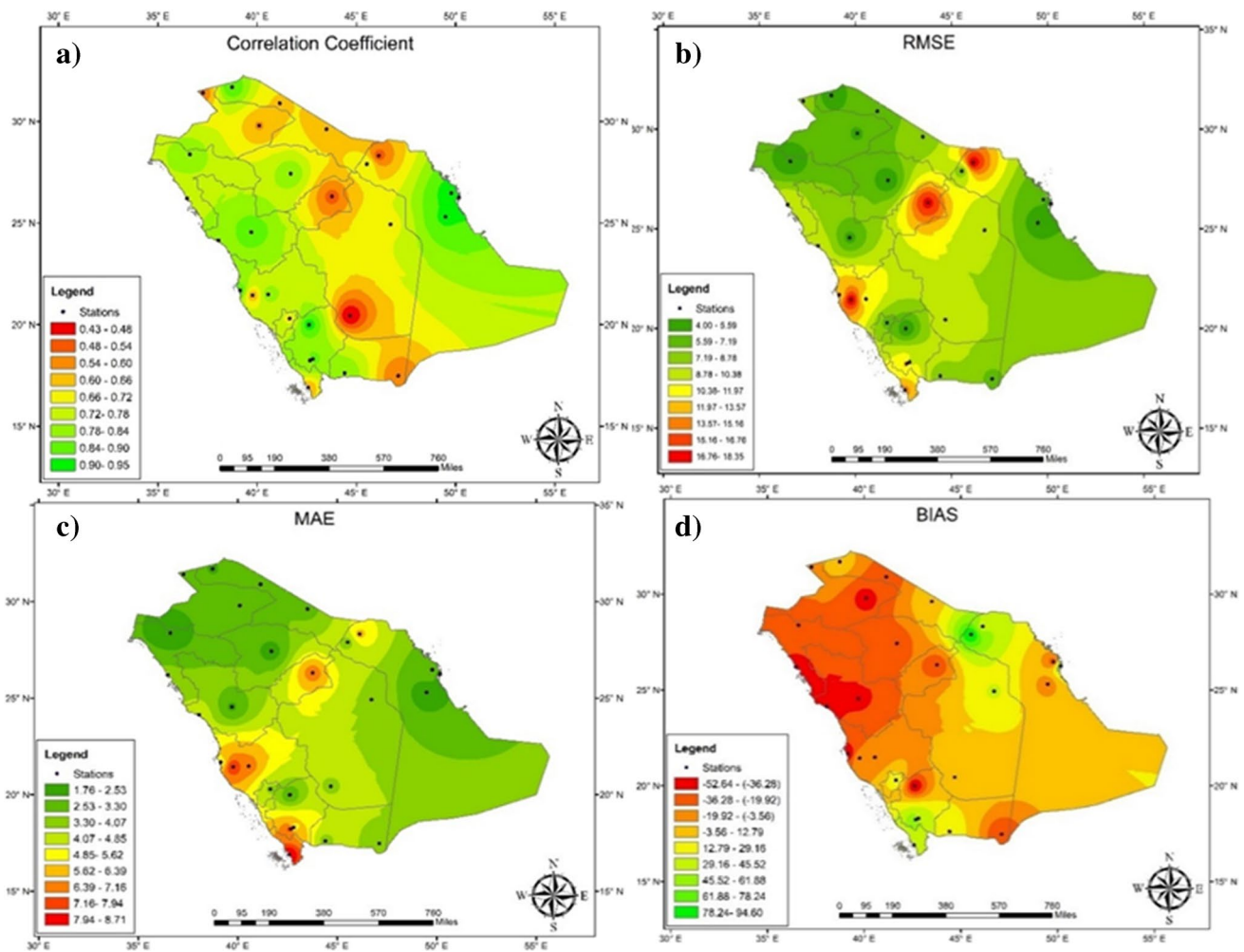


**Fig. 8** Station-based spatial distribution statistical performance measures between rainfall ground stations and TRMM: **a** CC, **b** RMSE, **c** MAE, and **d** BIAS

regional-based and station-based. The regional-based evaluation indicated the performance versus ground station data on a regional scale (13 regions in KSA), whereas the station-based examination provided information about each station (28 stations). Regression and correlation analysis provided a functional relationship between both datasets that have been developed and presented in Table 4. The highest  $R^2 = 0.92$  for the Dhahran station and the lowest  $R^2 = 0.2$  for Wadi Dawasir station. RMSE and MAE are the error indicators that showed high values for Makkah (RMSE = 18.4 mm, MAE = 8.03 mm), Jazan (RMSE = 14 mm, MAE = 8.72 mm), and Qassim (RMSE = 17.3 mm, MAE = 6.8 mm), while the minimum values were at Tabuk (RMSE = 4.3 mm, MAE = 1.76 mm) and Hail (RMSE = 4.5 mm, MAE = 2.23 mm). Likewise, R.B. indicated overestimation and underestimation between ground and satellite data. R.B. showed a higher percentage for most of the regions. The maximum

overestimation occurred at Hafar Al-Batin (R.B. = 94.6%), while the minimum overestimation occurred at Wadi-Dawasir (R.B. = 7.5%). However, the maximum underestimation occurred at Jeddah (R.B. = -52.8%), while the minimum underestimation occurred at Qurayyat (R.B. = -5.9%).

The station-based evaluation was also gone through the same statistical analysis. Regression and correlation indices showed excellent behavior in the stations of Asir and the Eastern region, while moderate behavior was found in southern and southwestern observatories and lowest at mixed locations in most of the southern and northern sides. Similarly, higher R.B. was observed for most southern and eastern parts, while lower at north and south-western stations. Overall, the results indicated a moderate behavior of the TRMM satellite to observe rain over Saudi Arabia. However, more promising studies for the Kingdom with higher ground observations and longer periods are recommended to explore further satellite performance.

**Table 4** Statistical indices for each station ( $R^2$ , RMSE, MAE, %BIAS, and CC)

Region	Station	Regression equation	$R^2$ station	RMSE (mm)	MAE (mm)	BIAS %	CC
Asir	Abha	$y = 1.1128x + 3.50$	0.67	12.8	7.89	68.8	0.81
	Khamis Mushait	$y = 0.6341x + 2.50$	0.77	9.4	4.78	30.4	0.88
	Bisha	$y = 0.9811x + 1.57$	0.87	4.0	2.50	-51.3	0.93
Najran	Najran	$y = 0.7476x + 2.50$	0.7	7.8	3.82	18.0	0.84
	Sharorah	$y = 0.4418x + 2.17$	0.31	6.9	3.32	-34.4	0.55
Jazan	Jazan	$y = 0.7802x + 7.10$	0.4	14.0	8.72	44.6	0.62
Al-Baha	Baha	$y = 0.5685x + 2.59$	0.51	6.8	3.99	26.0	0.71
	Taif	$y = 0.9369x + 4.35$	0.66	11.1	6.70	-18.3	0.81
Makkah	Makkah	$y = 0.7485x + 3.34$	0.41	18.4	8.03	-2.9	0.61
	Jeddah	$y = 1.3014x + 2.27$	0.8	12.0	5.29	-52.8	0.89
Riyadh	Riyadh	$y = 0.5988x + 2.05$	0.51	9.4	4.07	30.8	0.71
	Wadi Dawasir	$y = 0.3027x + 2.25$	0.2	9.9	3.95	7.5	0.43
	Hafar Al-Batin	$y = 0.8432x + 1.74$	0.54	7.6	3.83	94.6	0.73
	Qaisumah	$y = 0.2735x + 3.62$	0.28	18.1	5.84	41.1	0.52
Eastern Region	Al-Ahsa	$y = 0.8434x + 0.75$	0.83	4.9	1.92	-13.1	0.91
	Dhahran	$y = 0.8299x + 1.61$	0.92	4.2	2.14	64.8	0.96
	Dammam	$y = 0.8847x + 2.00$	0.85	6.1	3.33	-31.2	0.92
Madinah	Madina	$y = 0.7573x + 1.73$	0.79	5.2	2.42	-39.1	0.89
	Yanbu	$y = 0.4493x + 2.96$	0.67	9.5	4.39	-41.9	0.82
Al-Jouf	Jawf	$y = 0.7916x + 2.46$	0.35	5.5	3.06	-44.2	0.6
	Qurayyat	$y = 0.6465x + 2.55$	0.33	8.3	3.11	-5.9	0.57
Tabuk	Tabuk	$y = 0.9428x + 1.02$	0.67	4.3	1.76	-27.2	0.82
	Wajh	$y = 0.3153x + 1.97$	0.55	10.4	3.39	-39.5	0.74
	Hail	$y = 0.7257x + 1.57$	0.69	4.5	2.23	-30.9	0.83
Northern Border	Arar	$y = 1.156x + 1.98$	0.43	6.4	3.07	-30.0	0.66
	Rafha	$y = 1.0285x + 1.46$	0.4	7.4	3.09	9.6	0.63
	Turaif	$y = 0.8119x + 0.78$	0.82	4.7	2.49	8.9	0.9
Qassim	Qassim	$y = 0.7095x + 5.28$	0.29	17.3	6.80	-29.8	0.53

$y$  monthly satellite rainfall (mm),  $x$  monthly ground station rainfall (mm)

**Fig. 9** The variability of  $R^2$  with the elevation of the rain gauges

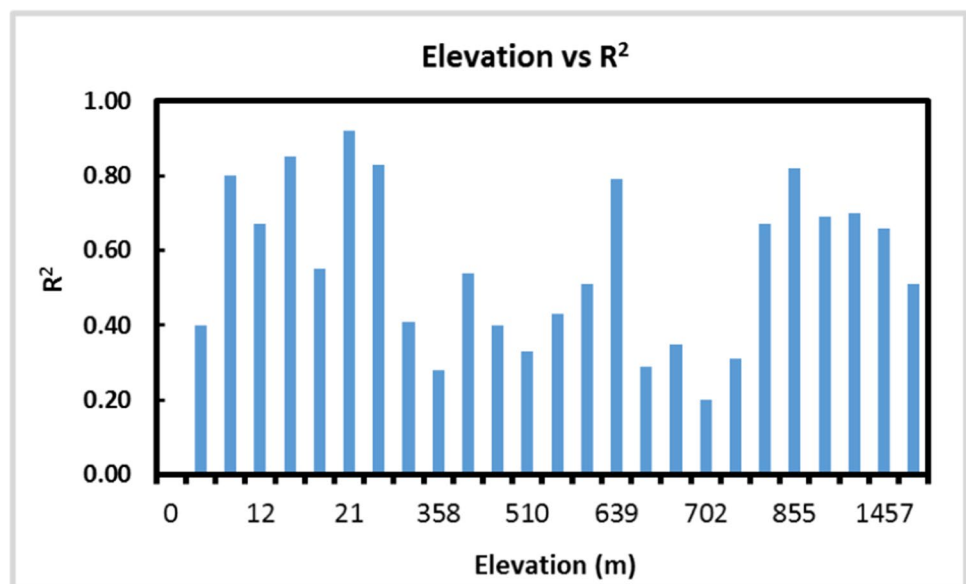
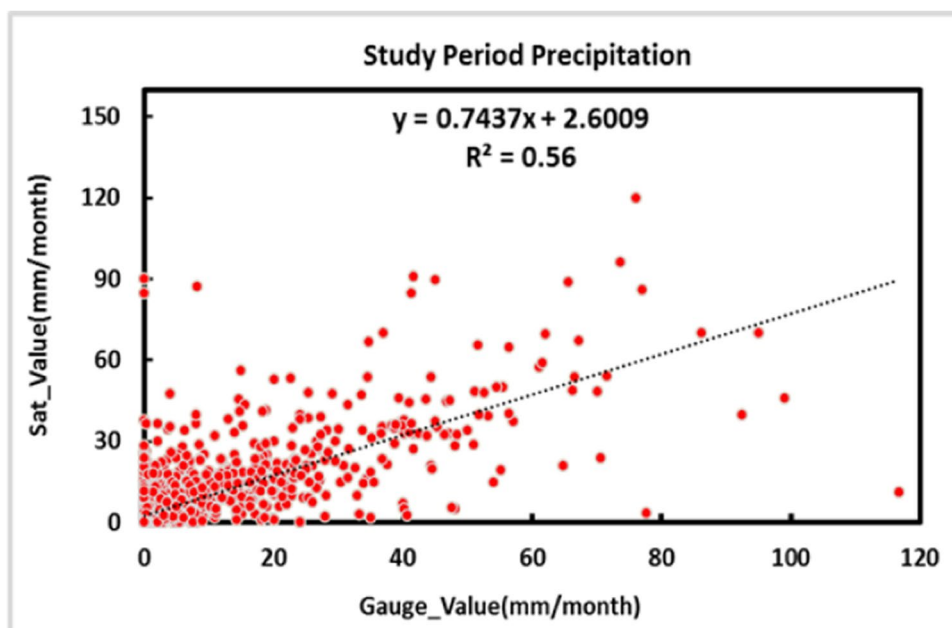




**Fig. 10** Scatter plot and regression analysis of monthly rainfall from the study stations



**Acknowledgements** This project was funded by the Deanship of Scientific Research (DSR), King Abdulaziz University, Jeddah, under Grant No. (G-51-155-1442). The authors, therefore, acknowledge with thanks, DSR technical, and financial support.

**Author contribution** Conceptualization, A. E. and M. E.; methodology, S. H. and A. C.; validation, E. A., A. E., and S. H.; formal analysis, S. H. and M. E.; writing—original draft preparation, A. E., M. E., and A. C.; writing—review and editing, A. E., M. E., and S. H.

**Funding** This research was funded by The Chinese Academy of Sciences (CAS), President's International Fellowship Initiative (PIFI), grant number 2021VEA0007.

**Data availability** All data generated or analyzed during this study are included in this published article.

**Code availability** All codes for data cleaning and analysis associated with the current submission are available at the local authorities in Saudi Arabia.

## Declarations

**Ethics approval** For this type of study, formal approval is not required.

**Consent to participate** For this type of study, formal consent is not required.

**Consent for publication** For this type of study, consent for publication is not required.

**Conflict of interest** The authors declare no competing interests.

## References

- Abdullah M, Al-Mazroui M (1998) Climatological study of the southwestern region of Saudi Arabia I Rainfall Analysis. *Clim Res* 9:213–223
- Abera W, Brocca L, Rigon R (2016) Comparative evaluation of different satellite rainfall estimation products and bias correction in the Upper Blue Nile (UBN) basin. *Atmos Res* 178:471–483
- Alharthi A, El-Sheikh MA, Elhag M, Alatar AA, Abbadi GA, Abdel-Salam EM, Arif IA, Baeshen AA, Eid EM (2020) Remote sensing of 10 years changes in the vegetation cover of the northwestern coastal land of Red Sea, Saudi Arabia. *Saudi J Biosoc Sci* 27(11):3169–3179
- Almazroui M (2011) Calibration of TRMM rainfall climatology over Saudi Arabia during 1998–2009. *Atmos Res* 99:400–414
- Artan G, Gadain H, Smith JL, Asante K, Bandaragoda CJ, Verdin JP (2007) Adequacy of satellite derived rainfall data for stream flow modeling. *Nat Hazards* 43:167–185
- Awais M, Li W, Cheema MJM, Hussain S, AlGarni TS, Liu C, Ali A (2021) Remotely sensed identification of canopy characteristics using UAV-based imagery under unstable environmental conditions. *Environ Technol Innov* 22:101465
- Awais M, Li W, Hussain S, Cheema MJM, Li W, Song R, Liu C (2022) Comparative evaluation of land surface temperature images from unmanned aerial vehicle and satellite observation for agricultural areas using in situ data. *Agriculture* 12:184
- Bahrawi JA, Elhag M (2020) Consideration of seasonal variations on water radiometric indices estimation of soil moisture

- content in arid environment in Saudi Arabia. *Desalin Water Treat* 176:201–212
- Bahrawi J, Ewea H, Kamis A, Elhag M (2020) Potential flood risk due to urbanization expansion in arid environments, Saudi Arabia. *Nat Hazards* 104:795–809
- Bahrawi J, Alqarawy A, Chabaani A, Elfeki A, Elhag M (2021) Spatiotemporal analysis of the annual rainfall in the Kingdom of Saudi Arabia: predictions to 2030 with different confidence levels. *Theoret Appl Climatol* 146:1479–1499
- Behrangi A, Khakbaz B, Jaw TC, AghaKouchak A, Hsu K, Sorooshian S (2011) Hydrologic evaluation of satellite precipitation products over a mid-size basin. *J Hydrol* 397:225–237
- Camberlin P, Barraud G, Bigot S, Dewitte O, Makanzu Imwangana F, Maki Mateso JC, Martiny N, Monsieurs E, Moron V, Pellarin T (2019) Evaluation of remotely sensed rainfall products over Central Africa. *Q J R Meteorol Soc* 145:2115–2138
- Choubin B, Khalighi-Sigaroodi S, Mishra A, Goodarzi M, Shamshirband S, Ghaljaee E, Zhang F (2019) A novel bias correction framework of TMPA 3B42 daily precipitation data using similarity matrix/homogeneous conditions. *Sci Total Environ* 694:133680
- Collischonn B, Collischonn W, Tucci CEM (2008) Daily hydrological modeling in the Amazon basin using TRMM rainfall estimates. *J Hydrol* 360:207–216
- De Coning E (2013) Optimizing satellite-based precipitation estimation for nowcasting of rainfall and flash flood events over the South African domain. *Remote Sens* 5:5702–5724
- Dinku T, Ruiz F, Connor SJ, Ceccato P (2010) Validation and inter-comparison of satellite rainfall estimates over Colombia. *J Appl Meteorol Climatol* 49:1004–1014
- Elhag M (2016) Inconsistencies of SEBS model output based on the model inputs: global sensitivity contemplations. *J Indian Soc Remote* 44:435–442
- Elhag M, Yilmaz N (2021) Insights of remote sensing data to surmount rainfall/runoff data limitations of the downstream catchment of Pineios River, Greece. *Environ Earth Sci* 80:1–13
- Elhag M, Galal HK, Alsubaie H (2017) Understanding of morphometric features for adequate water resource management in arid environments. *Geosci Instrum Methods Data Syst* 6:293–300
- Elhag M, Gitas I, Othman A, Bahrawia J (2020) Effect of water surface area on the remotely sensed water quality parameters of Baysh Dam Lake, Saudi Arabia. *Desalin Water Treat* 194:369–378
- Elhag M, Bahrawi J, Boteva S (2021a) Input/output inconsistencies of daily evapotranspiration conducted empirically using remote sensing data in arid environments. *Open Geosciences* 13:321–334
- Elhag M, Gitas I, Othman A, Bahrawi J, Psilovikos A, Al-Amri N (2021b) Time series analysis of remotely sensed water quality parameters in arid environments, Saudi Arabia. *Environ Dev Sustain* 23:1392–1410
- Fang G, Yang J, Chen Y, Zammit C (2015) Comparing bias correction methods in downscaling meteorological variables for a hydrologic impact study in an arid area in China. *Hydrol Earth Syst Sci* 19:2547–2559
- Farran MM, Elfeki A, Elhag M, Chaabani A (2021) A comparative study of the estimation methods for NRCS curve number of natural arid basins and the impact on flash flood predications. *Arab J Geosci* 14:1–23
- Gado TA, Hsu K, Sorooshian S (2017) Rainfall frequency analysis for ungauged sites using satellite precipitation products. *J Hydrol* 554:646–655
- Gu H-h, Yu Z-b, Yang C-g, Ju Q, Lu B-h, Liang C (2010) Hydrological assessment of TRMM rainfall data over Yangtze River Basin. *Water Sci Eng* 3:418–430
- Gupta G, Ratnam MV, Madhavan B, Prasad P, Narayanamurthy C (2021) Vertical and spatial distribution of elevated aerosol layers obtained using long-term ground-based and space-borne lidar observations. *Atmos Environ* 246:118172
- Habib E, Nasrollahi N (2009) Evaluation of TRMM-TMPA satellite rainfall estimates over arid regions. *AGUFM 2009:H12A–H2*
- Habib E, Haile AT, Sazib N, Zhang Y, Rientjes T (2014) Effect of bias correction of satellite-rainfall estimates on runoff simulations at the source of the Upper Blue Nile. *Remote Sens* 6:6688–6708
- Hag-elsafi S, El-Tayib M (2016) Spatial and statistical analysis of rainfall in the Kingdom of Saudi Arabia from 1979 to 2008. *Weather* 71:262–266
- Haile AT, Yan F, Habib E (2015) Accuracy of the CMORPH satellite-rainfall product over Lake Tana Basin in Eastern Africa. *Atmos Res* 163:177–187
- Hasanean H, Almazroui M (2015) Rainfall: features and variations over Saudi Arabia, a review. *Climate* 3:578–626
- Hussain S, Bahrawi J, Awais M, Elhag M (2022) Understanding the role of the radiometric indices in temporal evapotranspiration estimation in arid environments. *Desalin Water Treat* 256:221–234
- Jiang S, Ren L, Hong Y, Yong B, Yang X, Yuan F, Ma M (2012) Comprehensive evaluation of multi-satellite precipitation products with a dense rain gauge network and optimally merging their simulated hydrological flows using the Bayesian model averaging method. *J Hydrol* 452:213–225
- Jiang Q, Li W, Wen J, Qiu C, Sun W, Fang Q, Xu M, Tan J (2018) Accuracy evaluation of two high-resolution satellite-based rainfall products: TRMM 3B42V7 and CMORPH in Shanghai. *Water* 10:40
- Joyce RJ, Janowiak JE, Arkin PA, Xie P (2004) CMORPH: a method that produces global precipitation estimates from passive microwave and infrared data at high spatial and temporal resolution. *J Hydrometeorol* 5:487–503
- Khan SI, Hong Y, Wang J, Yilmaz KK, Gourley JJ, Adler RF, Brakenridge GR, Policelli F, HabibIrwin SD (2010) Satellite remote sensing and hydrologic modeling for flood inundation mapping in Lake Victoria basin: implications for hydrologic prediction in ungauged basins. *IEEE Trans Geosci Remote Sens* 49:85–95
- Kozu T, Kawanishi T, Kuroiwa H, Kojima M, Oikawa K, Kumagai H, Ki O, Okumura M, Nakatsuka H, Nishikawa K (2001) Development of precipitation radar onboard the Tropical Rainfall Measuring Mission (TRMM) satellite. *IEEE Trans Geosci Remote Sens* 39:102–116
- Kummerow C, Barnes W, Kozu T, Shiue J, Simpson J (1998) The tropical rainfall measuring mission (TRMM) sensor package. *J Atmos Ocean Technol* 15:809–817
- Kummerow C, Simpson J, Thiele O, Barnes W, Chang A, Stocker E, Adler R, Hou A, Kakar R, Wentz F (2000) The status of the Tropical Rainfall Measuring Mission (TRMM) after two years in orbit. *J Appl Meteorol* 39:1965–1982
- Liu Z, Ostrenga D, Teng W, Kempler S (2012) Tropical Rainfall Measuring Mission (TRMM) precipitation data and services for research and applications. *Bull Am Meteorol Soc* 93:1317–1325
- Lu D, Yong B (2018) Evaluation and hydrological utility of the latest GPM IMERG V5 and GSMaP V7 precipitation products over the Tibetan Plateau. *Remote Sens* 10:2022
- Maggioni V, Massari C (2018) On the performance of satellite precipitation products in riverine flood modeling: A review. *J Hydrol* 558:214–224
- Mahmoud MT, Al-Zahrani MA, Sharif HO (2018) Assessment of global precipitation measurement satellite products over Saudi Arabia. *J Hydrol* 559:1–12
- Moazami S, Golian S, Kavianpour MR, Hong Y (2013) Comparison of PERSIANN and V7 TRMM Multi-satellite Precipitation Analysis (TMPA) products with rain gauge data over Iran. *Int J Remote Sens* 34:8156–8171

- Poinsot P (2020) Jules Dupuit (1804–1866): Cost-benefit analysis and collective choices. *Great Minds in Regional Science*. Springer, pp 73–90
- Psilovikos A, Elhag M (2013) Forecasting of remotely sensed daily evapotranspiration data over Nile Delta region Egypt. *Water Resour Manag* 27:4115–4130
- Ricciardelli E, Di Paola F, Gentile S, Cersosimo A, Cimini D, Gallucci D, Gherardi E, Larosa S, Nilo ST, Ripepi E (2018) Analysis of Livorno heavy rainfall event: examples of satellite-based observation techniques in support of numerical weather prediction. *Remote Sens* 10:1549
- Segond M-L, Wheeler HS, Onof C (2007) The significance of spatial rainfall representation for flood runoff estimation: a numerical evaluation based on the Lee catchment, UK. *J Hydrol* 347:116–131
- Şen Z, Al-Suba'i K (2002) Hydrological considerations for dam siting in arid regions: a Saudi Arabian study. *Hydrol Sci J* 47:173–186
- Seyyedi H, Anagnostou EN, Beighley E, McCollum J (2014) Satellite-driven downscaling of global reanalysis precipitation products for hydrological applications. *Hydrol Earth Syst Sci* 18(12):5077–5091
- Su F, Gao H, Huffman GJ, Lettenmaier DP (2011) Potential utility of the real-time TMPA-RT precipitation estimates in streamflow prediction. *J Hydrometeorol* 12:444–455
- Swain DL, Singh D, Touma D, Diffenbaugh NS (2020) Attributing extreme events to climate change: a new frontier in a warming world. *One Earth* 2:522–527
- Tapiador F, Navarro A, Levizzani V, García-Ortega E, Huffman G, Kidd C, Kucera P, Kummerow C, Masunaga H, Petersen W (2017) Global precipitation measurements for validating climate models. *Atmos Res* 197:1–20
- Vu TT, Li L, Jun KS (2018) Evaluation of multi-satellite precipitation products for streamflow simulations: a case study for the Han River Basin in the Korean Peninsula. *East Asia Water* 10:642

**Publisher's note** Springer Nature remains neutral with regard to jurisdictional claims in published maps and institutional affiliations.